DD

GSI

GSI-Preprint-97-65
Oktober 1997

SCANNING FORCE MICROSCOPY ON HEAVY - ION TRACKS IN MUSCOVITE MICA: TRACK DIAMETER VERSUS ENERGY LOSS AND LOADING FORCE

J. Ackermann, A. Müller, R. Neumann, Y. Wang

(Accepted for publication in „Applied Physics A")

Gesellschaft für Schwerionenforschung mbH
Planckstraße 1 • D-64291 Darmstadt • Germany
Postfach 11 05 52 • D-64220 Darmstadt • Germany

Accepted for publication in: **Applied Physics A** (spring 1998)

Scanning force microscopy on heavy-ion tracks in muscovite mica: track diameter versus energy loss and loading force

J. Ackermann, A. Müller, R. Neumann, Y. Wang*

Gesellschaft für Schwerionenforschung Darmstadt (GSI), Planckstraße 1,

D-64291 Darmstadt, Germany

Phone: +49-6159-712172, FAX +49-6159-712179, E-Mail: r.neumann@gsi.de

(*Permanent Address: Institute of Heavy Ion Physics, Beijing University, Beijing 100871, P.R. of China)

Abstract

Mica is very sensitive to heavy-ion irradiation and offers also an ideal surface for scanning force microscopy (SFM) of ion-induced tracks. Mica samples were irradiated with heavy ions (the kinetic energies ranging from 0.5 to 2.76 GeV) at the Universal Linear Accelerator UNILAC of GSI. The cross sections of latent ion tracks on freshly cleaved mica surfaces were imaged by lateral-force microscopy. By evaluating the statistical distribution of the track diameters, we enlarged our previously available data set of mean track diameters versus ion energy loss by two additional points for zinc and selenium. The influence of the loading force on the SFM imaging process was also addressed confirming a linear relation between apparent ion track diameters and load.

PACS: 7.79.Sp; 61.80.Jh; 61.82.Ms

1. Introduction

In numerous solids, the passage of heavy ions with kinetic energies ranging from several hundred MeV to some GeV leads to dramatic, very rapidly developing changes of the original structure, e.g., the local amorphization of an insulating or semiconducting crystal along the ion trajectories. A uranium ion, to consider an extreme case, accelerated to a kinetic energy of 11.4 MeV/nucleon by the Universal Linear Accelerator UNILAC of GSI, moves over the first tens of microns of its path with about 15 % of the velocity of light. At this speed, the projectile transfers its energy almost exclusively by Coulomb interaction with the electrons of the target, successively depositing energy amounts in the order of 30 keV/nm in time intervals of $2 \cdot 10^{-17}$ seconds. The primary processes initiating and driving the changes cannot be observed directly. However, the characteristics of the remaining, irreversibly altered zones (in the case of continuous damage trails called latent tracks) such as size, shape, and internal structure contain indirect information about these processes. Detailed studies of track morphology and dimensions as a function of different parameters, in particular energy loss or physical and chemical material properties, are required. A comprehensive understanding of damage formation by energetic ion projectiles can be achieved only on a long-term basis by collecting data from many different materials and by accompanying the experimental findings with gradually refined modelling [see, e.g., 1, 2, and refs. therein].

It was early recognized that the mineral muscovite mica is very sensitive to irradiation with energetic heavy ions. Over several decades, ion tracks in this material have therefore been investigated with different techniques. First studies with transmission electron microscopy (TEM) [3-5] were followed by works on small-angle X-ray [6-9] and neutron scattering [8]. Such X-ray and neutron experiments require typically 10^{10}-10^{11} ion tracks, serving as scattering centres in order to produce a signal pattern. More recently, several groups focused on the visualization of single individual tracks by applying a variety of imaging modes of scanning force microscopy (SFM) [10-19].

In scanning-force micrographs of high resolution, the cross sections of latent tracks in mica appear as circular zones without any atomic order, that are surrounded by the intact crystalline lattice. Obviously, the material is fully amorphized within a narrow cylindrical volume along the trajectory of the heavy-ion projectile. Besides imaging the topography of a surface, SFM offers the possibility of simultaneously mapping the dynamic friction coefficient. It was found that the track cross sections on the surface of freshly cleaved mica samples possess a remarkably higher friction than the undamaged crystal [12, 17]. Furthermore, force modulation measurements revealed the damaged areas being softer than their intact surroundings [18].

The findings mentioned before illustrate that heavy-ion tracks in mica represent objects of extremely small size, embedded in an environment of very different structure. Therefore, they are particularly suited for SFM studies of surface properties such as friction and hardness (or elasticity) on a nanometer scale. Moreover, they provide access to problems concerning the convolution of features of sample and force sensor. Thus, by variation of the loading force, the tracks can also be used to study the influence of the tip-sample contact area on the imaging process.

In the present work, we focus mainly on two subjects: Firstly, we report further data points near the threshold of ion-track creation that enlarge our data set of track diameters in mica measured by lateral-force microscopy. Secondly, we discuss results on the increase of the apparent track-diameter with increasing loading force.

2. Experimental results and discussion

2.1 General remarks

Muscovite mica is an insulating, layered crystalline silicate. It is easily cleavable and splits always between the two adjacent SiO_4 (001) lattice planes. The SiO_4 tetrahedra form an hexagonal pattern that has been studied comprehensively by SFM [20-22].

For the purpose of ion track studies, we irradiated mica samples under normal incidence (perpendicular to the (001) planes) with different heavy ion species at the UNILAC. Above a certain threshold, each impinging projectile creates a latent track. The loss dE/dx of projectile energy per unit path length can be calculated with the *transport of ions in matter* (TRIM) code [23]. When plotted as a function of penetration depth, dE/dx shows a broad plateau, slightly increasing from the value given at the sample surface to the so-called Bragg maximum, that is followed by a steep fall-off to zero.

Pulling off a thin mica sheet with an adhesive tape provides a fresh surface plane suitable for highly resolved SFM imaging. Several surface layers with a thickness of some microns can be removed before leaving the energy-loss plateau. After cleavage, the samples were examined in air with a homebuilt scanning force microscope. We used commercial bar-shaped as well as V-shaped Si_3N_4 cantilevers (Park Scientific Instruments) with different dimensions and spring constants. Each cantilever was equipped with a pyramidal tip, having a flat area at its end with a diameter of several tens of nanometers, as we concluded from scanning electron microscopy images. We assume, however, that a tip usually possesses at its very front a rough uneven surface with nanometer-sized asperities.

As an example, a lateral-force image of several gold ion tracks in mica is shown in Fig. 1a. Low brightness represents a high lateral force and vice versa. It should be emphasized that the micrograph displays the friction-dominated lateral force and not the topography. The track cross sections exhibit a larger friction than the surrounding intact surface. It was found that the topographic level of the cross sections coincided fully with the cleaved surface planes, exhibiting neither craters nor hillocks. In contrast to this, the ions created hillocks on the original sample surface [19].

2.2 Determination of ion track diameters

To extract the diameter of an individual track, its lateral-force profile normal to the fast scanning direction was evaluated by determining a left (F_l) and a right (F_r) foot (Fig. 1b). The track boundary was defined by the transition from the amorphized region to its crystalline

surroundings. Mean diameters for the different ion species were obtained by fitting the diameter distributions with a Gaussian curve. Fig. 2 displays our measurements of latent-track diameters in mica (black dots) as a function of dE/dx, together with the results from topographic SFM imaging [10, 11] and small-angle X-ray and neutron scattering [6-9]. From left to right our data points are related to irradiation with the following ion species, the total kinetic energies in units of GeV being added in brackets: zinc (0.78), selenium (0.91), krypton (0.5), xenon (1.47), gold (2.64), lead (2.37), and uranium (2.76). The points for zinc and selenium enlarge our previously available data set, already given in ref. [17].

Our vertical error bars of ±2 nm are not statistical, but were chosen in order to take into account the problem of determining the border line between the disordered track region and the undamaged crystalline lattice. The horizontal error bars reflect the fact, that the energy-loss plateau is not exactly horizontal, but increases slightly as a function of depth. Usually, each sample was cleaved repeatedly, when collecting the data required for a given mean diameter. Therefore, the plateau range passed through by several cleavage procedures, determines the uncertainty of the dE/dx-abscissa values.

The three sets of diameters are in good agreement for low dE/dx values, but develop clear discrepancies with increasing ion energy loss. These deviations may partially originate from different definitions of the track diameter entering the evaluation procedures. A full clarification, however, will require further thorough investigations. A more detailed discussion of the evaluation procedures applied by the different groups is given in ref. [17]. Recently, a fourth set of mean track diameters in mica was achieved by TEM measurements [24].

2.3 Apparent ion track diameters vs. loading force

In a previous SFM work, we had studied the average friction force versus the loading force both on the undamaged mica surface and inside the ion-track cross sections [12]. We found a linear dependence (as expressed by Amontons' law) in both areas, and a significantly larger sliding-friction coefficient inside the track zone than on the intact lattice. When collecting our first data on ion track diameters [12], the SFM images indicated also a slight increase of the

track diameters with increasing load. However, since we performed the measurements at loading forces not larger than about 30 nN, the possible error was assumed to be covered by the ±2 nm error bars. In the present work, we investigated the dependence of the apparent track diameters on the loading force in more detail.

The cross sections of selenium and gold ion tracks were measured at different loading forces, analyzing several tens of individual tracks for each data point. The averaged diameters were extracted by fitting the distributions with a Gaussian curve; the result is displayed in Fig. 3. Here, zero load is defined by the point in the loading force-to-distance curve at which the cantilever experiences no force and is therefore free of bending [25]. The symbols have about the size of the vertical $\pm 1\sigma$-uncertainties resulting from the Gaussian fit. The straight lines represent fits to the data points. If only the functional behaviour of the diameter-to-load relation is considered, it makes no sense to provide the single points with a ±2 nm error bar, since all points have been acquired with the same imaging and evaluation method. However, one should attribute ±2 nm to the crossing point of a linear fit curve and the ordinate, when identifying it with the actual mean diameter (as if measured with zero load).

Obviously, the size of the preset loading force has a non-negligible influence on the imaging process. When operating the force microscope in the contact mode, there always exists a contact area between probe tip and sample. Assuming the validity of Amontons' law, as concluded from the linear relation of sliding-friction force and load on mica [12], the contact area between probe tip and sample grows linearly with increasing loading force, and via a convolution with the track cross section enlarges the apparent diameter of the amorphized zone. This model is illustrated qualitatively in Fig. 4. As long as the contact area (possibly realized by a single-asperity contact) is significantly smaller than the track cross section, the broadening should result mainly from the overlap near the track boundary. This assumption is supported by the finding that the FWHM-diameter of the tracks is independent of the applied force (data symbolized by o in Fig. 3). A linear increase of the mean track diameter as a function of loading force was also reported by Seider et al. [26] for 500 MeV Xe-tracks in mica. One should be aware, however, that the functional behaviour of the track diameter-versus-load curves depends on parameters such as microcorrugation of the probe tip and capillary forces, and may also

deviate from a straight line. Schwarz et al. [27, 28] discussed these implications of the probe-sample contact area in more detail within the framework of a generalized Hertzian theory.

3. Conclusions

The mean ion track diameters as a function of energy loss measured by SFM and small-angle X-ray and neutron scattering agree well for low dE/dx up to about 12-15 keV/nm, but show increasing discrepancies for higher dE/dx. Thus, further SFM measurements, preferably under ultrahigh-vacuum conditions and with different imaging modes such as the non-contact mode are highly desirable. Moreover, a comparison with recently achieved TEM results [24] should be helpful for a final clarification of the present differences. Ion track cross sections have proven to be also objects especially suitable for studies of SFM imaging parameters on the nanometer scale. Detailed measurements of the functional dependence of track diameters on the loading force under well-defined conditions, including ultrahigh vacuum and a very sharp tip could contribute to the experimental basis necessary for crucial tests of the Hertzian theory on a microscopic scale. [see, e.g., 27, 28, and refs. therein].

Acknowledgements. One of the authors (Y. W.) thanks GSI for financial support during his stay in Darmstadt from January to August 1996. Fruitful discussions with S. Bouffard (CIRIL, Caen, France) and U.D. Schwarz (Univ. of Hamburg, Germany) are also gratefully acknowledged.

References

[1] M. Toulemonde, C. Dufour, E. Paumier: *Phys. Rev.* ***B 46***, 14362 (1992)

[2] A. Meftah, F. Brisard, J.M. Costanini, E. Dooryhee, M. Hage-Ali, M. Hervieu, J.P. Stoquert, F. Studer, M. Toulemonde: *Phys. Rev.* ***B 49***, 12457 (1994)

[3] E.C.H. Silk, R. S. Barnes: *Phil. Mag.* ***4***, 211 (1959)

[4] G. Bonfiglioli, A. Ferro, A. Mojoni: *J. Appl. Phys.* ***32***, 2499 (1961)

[5] P.B. Price, R.M. Walker: *Phys. Rev. Lett.* ***8***, 217 (1962)

[6] E. Dartyge, M. Lambert: *Radiat. Eff.* ***21***, 71 (1974)

[7] E. Dartyge, J.P. Duraud, Y. Langevin, M. Maurette: *Phys. Rev.* ***B 23***, 5213 (1981)

[8] D. Albrecht, P. Armbruster, R. Spohr, M. Roth, K. Schaupert, H. Stuhrmann: *Appl. Phys.* ***A 37***, 37 (1985)

[9] D. Albrecht, E. Balanzat, K. Schaupert: *Nucl. Tracks Radiat. Meas.* ***11***, 93 (1986)

[10] F. Thibaudau, J. Cousty, E. Balanzat, S. Bouffard: *Phys. Rev. Lett.* ***67***, 1582 (1991)

[11] S. Bouffard, J. Cousty, Y. Pennec, F. Thibaudau: *Radiat. Eff. Def. Sol.* ***126***, 225 (1993)

[12] T. Hagen, S. Grafström, J. Ackermann, R. Neumann, C. Trautmann, J. Vetter, N. Angert: *J. Vac. Sci. Technol.* ***B 12***, 1555 (1994)

[13] J. Ackermann, N. Angert, S. Grafström, T. Hagen, M. Neitzert, R. Neumann, C. Trautmann, in: *Forces in Scanning Probe Methods* (eds. H.-J. Güntherodt, D. Anselmetti and E. Meyer), Kluwer Academic Publishers (1995), p. 489

[14] D.D.N.B. Daya, A. Hallén, P. Håkansson, B.U.R. Sundqvist, C.T. Reimann: *Nucl. Instr. and Meth.* ***B 103***, 454 (1995)

[15] D.D.N.B. Daya, A. Hallén, J. Eriksson, J. Kopniczky, R. Papaléo, C.T. Reimann, A. Brunelle, S. Della-Negra, Y. Le Beyec: *Nucl. Instr. and Meth.* ***B 106***, 38 (1995)

[16] D.D.N.B. Daya, C.T. Reimann, B.U.R. Sundquist, P. Håkansson: *Nucl. Instr. and Meth.* ***B 111***, 87 (1996)

[17] J. Ackermann, N. Angert, R. Neumann, C. Trautmann, M. Dischner, T. Hagen, M. Sedlacek: *Nucl. Instr. and Meth.* ***B 107***, 181 (1996)

[18] R. Neumann, J. Ackermann, N. Angert, C. Trautmann, M. Dischner, T. Hagen, M. Sedlacek: *Nucl. Instr. and Meth.* ***B 116***, 492 (1996)

[19] J. Ackermann, S. Grafström, T. Hagen, Kowalski, R. Neumann, M. Sedlacek, in: *Micro/Nanotribology and its Applications*, (ed. B.Bushan), Kluwer Academic Publishers (1997), p. 261

[20] R. Erlandsson, G. Hadziioannou, C.M. Mate, G.M. McClelland, S. Chiang: *J. Chem. Phys.* ***89***, 5190 (1988)

[21] O. Marti, J. Colchero, J. Mlynek: *Nanotechnology* ***1***, 141 (1990)

[22] T.G. Sharp, P.I. Oden, P.R. Buseck: *Surf. Sci. Lett.* ***284***, L405 (1993)

[23] J.F. Ziegler, J.P. Biersack, U. Littmark: *The Stopping and Ranges of Ions in Solids*, Pergamon (1985)

[24] J. Vetter: Private communication

[25] R. Lüthi, E. Meyer, H. Haefke, L. Howald, W. Gutmannsbauer, M. Guggisberg, M. Bammerlin, H.-J. Güntherodt: *Surf. Sci.* ***338***, 247 (1995)

[26] M. Seider, U. D. Schwarz, R. Wiesendanger: *Phys. Rev.* ***B 53***, R16180 (1996)

[27] U.D. Schwarz, W. Allers, G. Gensterblum, R. Wiesendanger: *Phys. Rev.* ***B 52***, 14976 (1995)

[28] U.D. Schwarz, H. Bluhm, H. Hölscher, W. Allers, R. Wiesendanger, in: *The Physics of Sliding Friction*, (eds. B. N. J. Persson, E. Tosatti), Kluwer Academic Publishers (1996), p. 369

Figure Captions:

Fig. 1a. Lateral-force image (95·95 nm^2) of gold ion tracks in mica (with the fast-scanning direction from bottom to top). Low brightness represents a high lateral force and vice versa.

1b. Line scan from A to B across the amorphous track region marked by F_l and F_r.

Fig. 2. Diameters of latent ion tracks in mica versus energy loss.
(•) Our lateral-force SFM data.
(o) SFM [10, 11]
(x) Small-angle X-ray and neutron scattering [6-9].
The inset shows a magnification of the energy loss region containing the data points for zinc and selenium ions.

Fig. 3. Diameters of Au (x) and Se (•,o) ion tracks in mica as a function of loading force: Evaluation of F_l and F_r (x,•) and full width at half maximum (o). The vertical $\pm 1\sigma$-error bars are omitted since they have approximately the size of the symbols.

Fig. 4. Schematic of an apparent ion track diameter, depending on the loading force via the load-dependent size of the tip-sample contact area.

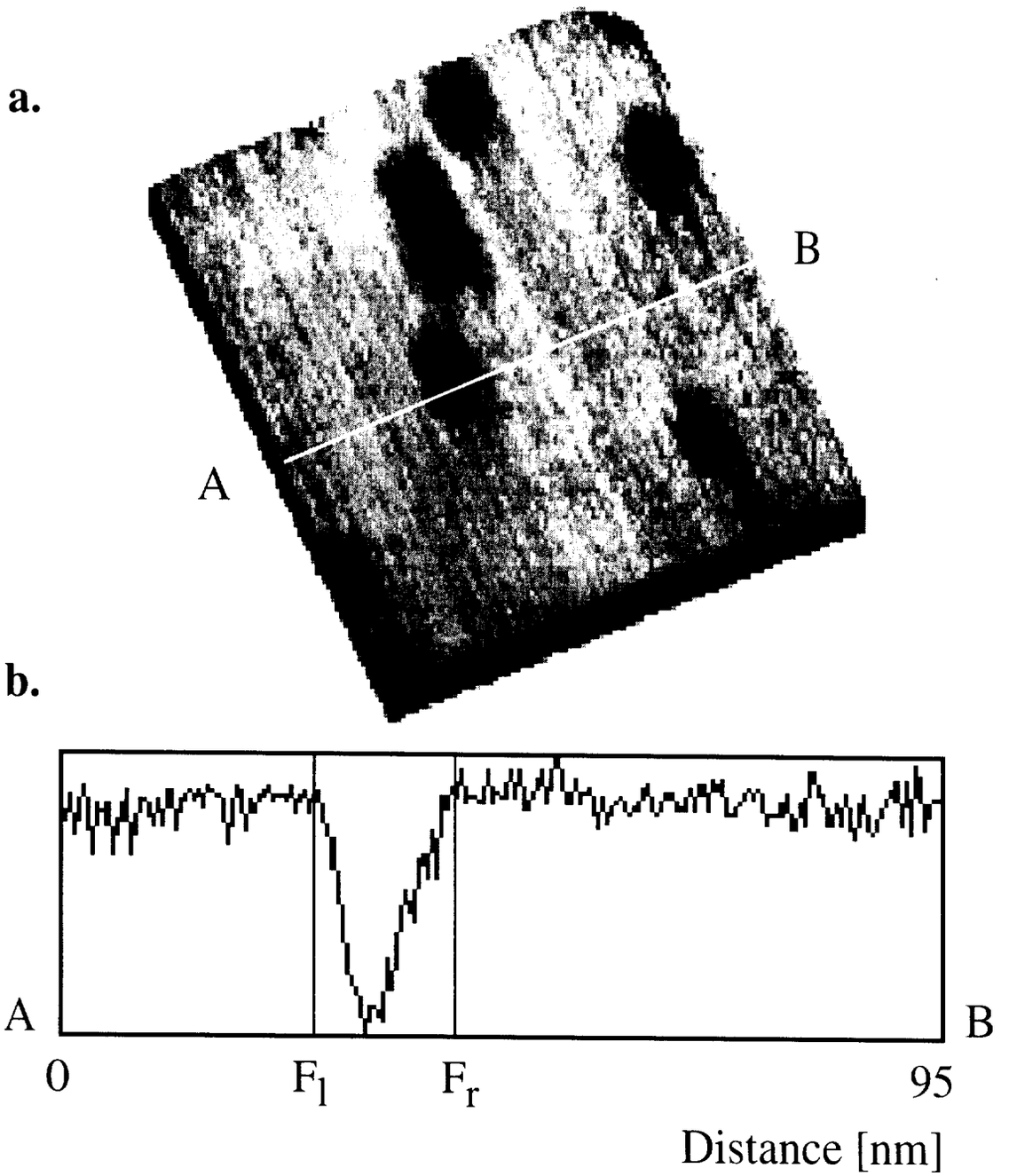

Fig. 1

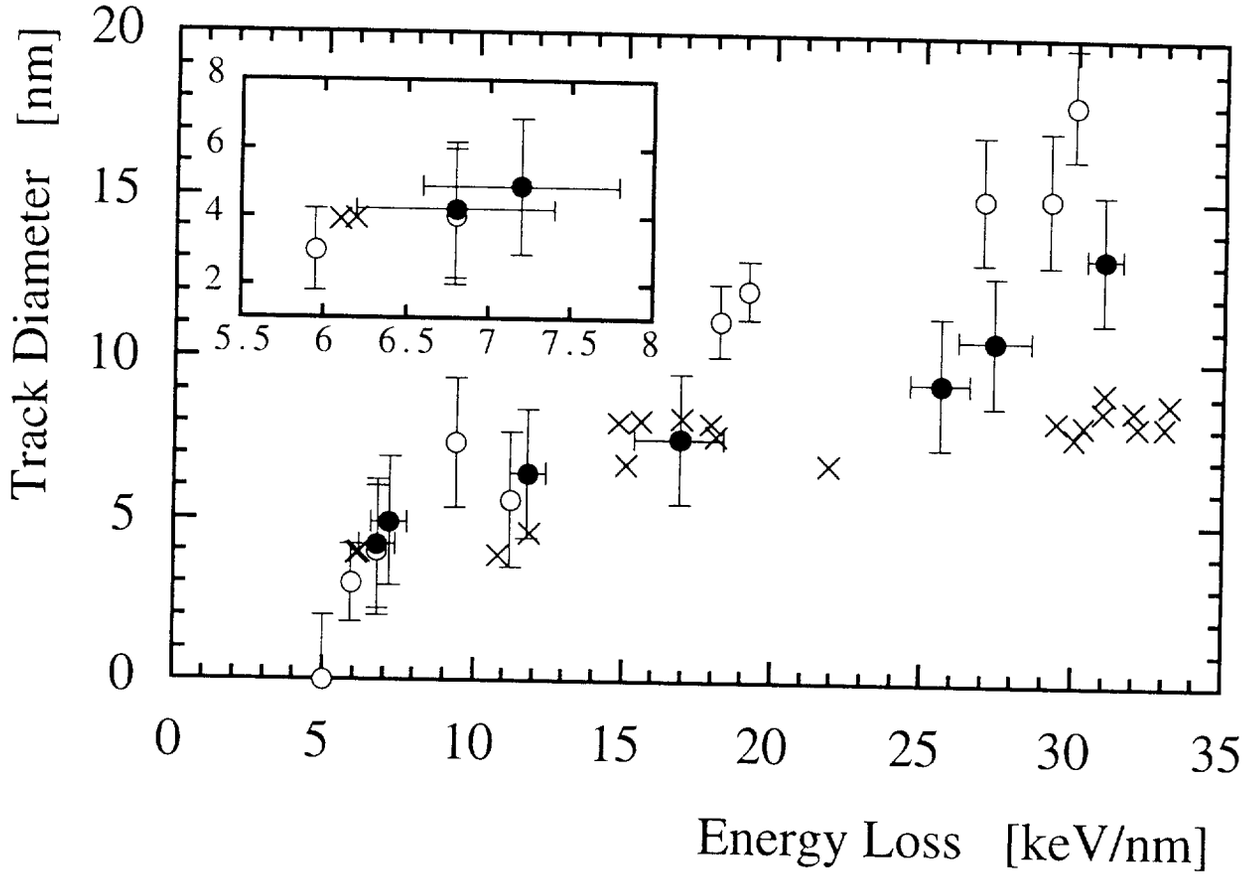
Track Diameter [nm]
20
15
10
5
0
0
5
10
15
20
25
30
35
Energy Loss [keV/nm]
8
6
4
2
5.5
6
6.5
7
7.5
8

Fig. 2

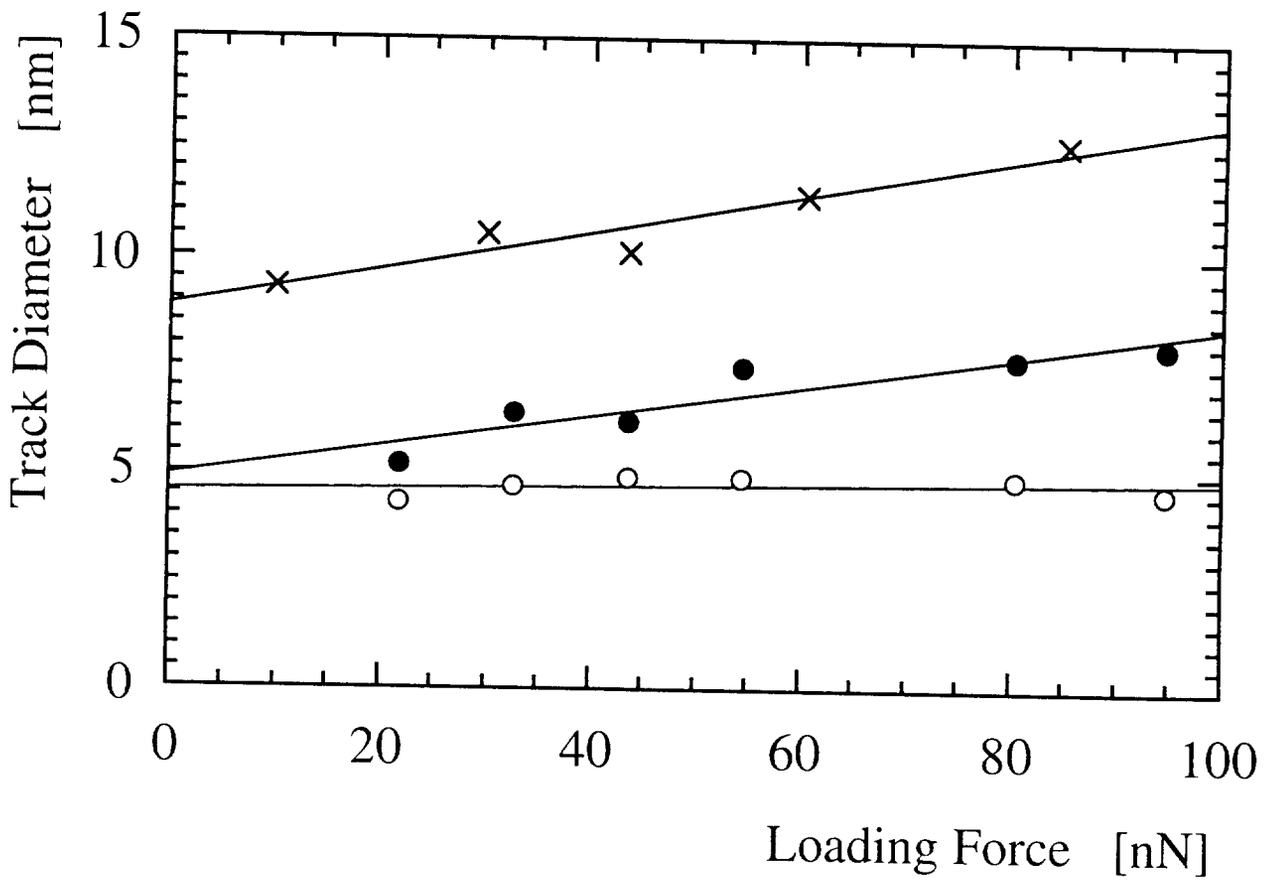

Fig. 3

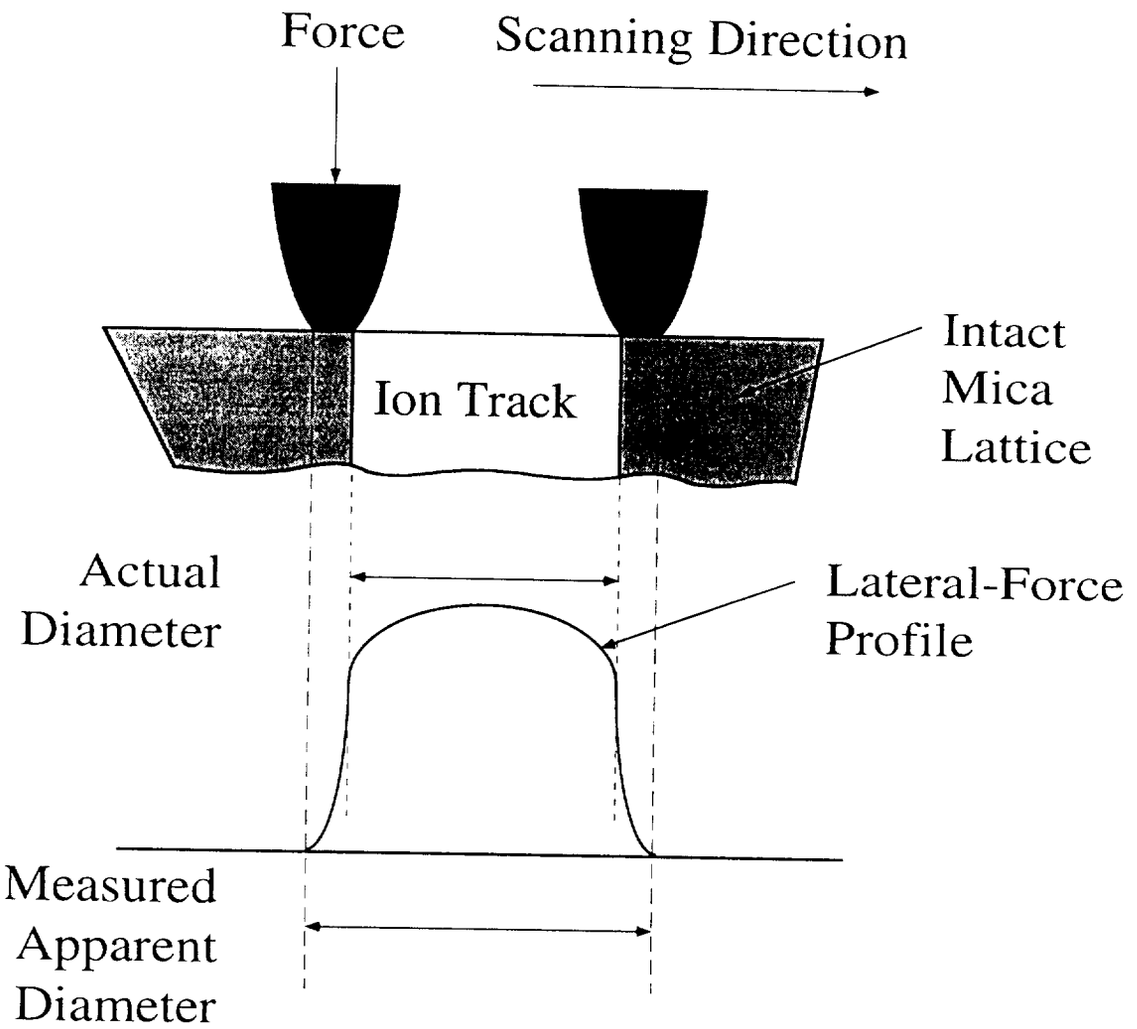
Force
Scanning Direction
Ion Track
Intact
Mica
Lattice
Actual
Diameter
Lateral-Force
Profile
Measured
Apparent
Diameter

Fig.4